

# Extended summary of doctoral thesis

# Optimization of polygeneration systems using hydrogen as an energy carrier

# Hamed Ghiasirad

Supervisor: Prof. Anna Skorek-Osikowska

Discipline: Environmental Engineering, Mining and Energy

Gliwice, Poland, 2025

#### Acknowledgements

I owe my deepest gratitude to my supportive supervisor, Prof. Anna Skorek-Osikowska, for her steadfast guidance, and generous encouragement throughout this work. I am especially grateful for her trust and for the inspiring research environment she fostered, one that I hope to continue contributing to after the PhD.

I also thank Towhid Gholizadeh for collaboration on our publications and projects, and Prof. Łukasz Bartela, Dr. Michał Jurczyk, and Jakub Ochmann for providing invaluable datasets and technical insights from the CAES energy storage experiments.

I am deeply grateful to my MSc supervisors, Prof. Rahim Khoshbakhti Saray and Dr. Siamak Mirmasoumi, for their guidance and for providing access to the experimental dataset from the anaerobic digestion system.

I gratefully acknowledge the formative LCA training received during my internships: at Karlstad University in Sweden with Dr. Ali Mohammadi and Dr. Farinaz Ebrahimian, and at Forschungszentrum Jülich in Germany with Dr. Christina Wulf.

I am profoundly grateful to my supportive family, whose encouragement helped me overcome life's challenges. I also thank all my colleagues at HMC and my Iranian friends in Gliwice. Without their companionship and support, living here would have been difficult.

I also wish to thank the Silesian University of Technology and the TrANsMIT COST Action CA21127 entitled Techno-economic analysis of carbon mitigation technologies for the awards and grants for accommodation, publications, my participation in internships, conferences, workshops, and training courses.

Finally, I gratefully acknowledge the support of the National Science Centre, Poland. Financial assistance was provided by grant no. 2021/41/B/ST8/02846 within the framework of the research project entitled Production of fuels and energy in the systems with negative CO2 emissions using high-temperature electrolysis and with oxygen management.

#### 1. Introduction

The EU has cut greenhouse-gas emissions to 3.2 GtCO<sub>2</sub>-eq in 2022, 31% below 1990, and is legally bound to at least –55% by 2030, –90% by 2040, and net-zero by 2050. Emissions are concentrated in energy-producing industries, transport, and other fuel combustion, with land use and forestry offsetting. In Poland, the energy industry dominates, while land use is a modest sink, underscoring the priority of power-sector decarbonization. The 2030 policy package centers on a tighter EU ETS, a strengthened Renewable Energy Directive, an economy-wide efficiency target, burden-sharing, and enhanced land-sector removals. Implementation spans coal/lignite phase-out; rapid build-out of renewables, storage, and grids; electrification and carbon capture in industry; low-carbon fuels in aviation and shipping; and replacing fossil hydrogen with renewable hydrogen. Together, accelerated renewable deployment and green hydrogen emerge as the most decisive, system-level levers for meeting the EU's 2030 climate goals [1].

#### 1.1. Renewable energy

The EU's policy framework, binding renewable targets, supportive regulation, and dedicated funding, has accelerated a structural shift away from fossil fuels toward wind, solar, and hydropower, complemented by nuclear as a stable, low-carbon source. The power mix is now dominated by low-emission generation, evidencing a clear decline in coal, oil, and gas. Poland, however, lags the EU average, underscoring the need to expand renewables and modernize systems rapidly. Closing this gap would align with EU climate obligations, reduce reliance on carbon-intensive fuels, improve air quality, and strengthen long-term energy security. With EU instruments in place, Poland has a timely opportunity to upgrade its infrastructure and contribute more fully to a sustainable European energy system [1].

#### 1.2. Biomass conversion

Bioenergy underpins clean-hydrogen pathways by supplying renewable carbon and dispatchable energy streams well suited to polygeneration. Anaerobic digestion converts wet residues into biogas—usable directly or upgraded to renewable gas—and nutrient-rich digestate that enables fertilizer and material recovery, with co-captured CO<sub>2</sub> offering additional valorization. Complementing this, biomass and waste gasification yield a hydrogen-rich syngas that, once cleaned, feeds high-efficiency power, low-carbon fuels, and chemicals. Together, these routes create revenue-bearing co-products and integrate with hydrogen systems to strengthen techno-economic performance and accelerate decarbonization across power, transport, and industry [2].

# 1.3. Hydrogen production

Hydrogen is a strategic pillar of EU decarbonization, linking the integration of large-scale renewables to deep cuts in hard-to-abate sectors. As illustrated in Fig. 1, the system transitions from a fossil-dominated baseline to a fully clean supply, with renewable-powered electrolysis emerging as the principal source, bio-hydrogen (with/without CCS) providing dispatchable low-carbon output, and a limited bridging role for gas-CCS; in CCS pathways, CO2 is captured and permanently stored. A net-zero-aligned strategy, therefore, prioritizes rapid renewable build-out to scale flexible electrolysis, complemented by sustainably sourced bio-hydrogen with CO2 capture to deliver firm capacity and durable removals while phasing out unabated fossil routes. Together, these levers offer a resilient, system-level pathway to climate neutrality [3].

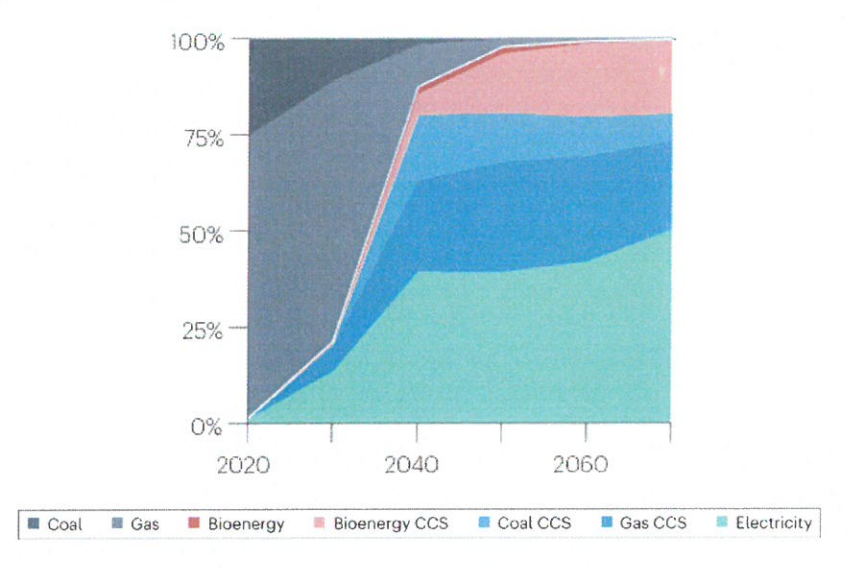


Fig. 1. Projections of hydrogen production methods to limit global warming to below 1.5 °C [3].

# 1.4. Hydrogen production using electrolysis cells

Alkaline electrolyzer offers the lowest capital cost but limited turndown; proton-exchange membrane (PEM) is compact, pressurizable, and highly responsive at comparable efficiency; solid-oxide electrolysis cell (SOEC), using steam and high-temperature operation, minimizes electricity use and enables reversible and co-electrolysis for direct e-fuel coupling, though durability under cycling remains a priority. These distinctions guide technology-to-application matching: alkaline for low-CAPEX baseload, PEM for grid-responsive duty, and SOEC as the strategic option where high-temperature heat is available for deeply integrated, lowest-energy green hydrogen and syngas production [4].

# 1.5. Hydrogen storage challenges

Direct hydrogen storage and logistics face inherent safety and materials challenges, flammability, cryogenics, leakage, embrittlement, and stringent siting and handling requirements, making large-scale deployment difficult. A more practical approach is to convert hydrogen immediately into denser, infrastructure-compatible carriers via power-to-X and biomass-to-X polygeneration. These derivatives are easier to store and transport, have lower operational risk, and integrate with existing fuel and chemical systems, preserving hydrogen's decarbonization value across hard-to-abate sectors [5].

# 1.6. Hydrogen applications

This section identifies priority demand centers that anchor the polygeneration configurations and optimization objectives for hydrogen. Near-term substitution focuses on replacing grey hydrogen in refining and hydrotreating, producing ammonia for fertilizers and as a carrier, and synthesizing methanol as a platform chemical and fuel. Additional high-impact uses include maritime and aviation fuels via power-to-X and biomass-to-X, low-carbon chemical feedstocks (including co-electrolysis routes), direct-reduced iron with electric arc furnaces, long-duration energy storage, and biogas upgrading through methanation. Together, these applications target hard-to-electrify segments and enable system-level decarbonization while leveraging hydrogen as both energy vector and carbon-integration agent.

# 2. Motivation and scope

This thesis demonstrates the feasibility of hydrogen-based polygeneration for liquid biofuels by integrating electrolysis, biomass conversion, synthesis loops, and utility systems to convert variable renewable energy sources into storable products. Specifically, it hypothesize that:

- It is possible to raise plant efficiency by adopting high-temperature electrolysis.
- It is possible to improve performance using oxy-fuel gas turbines with LNG regasification.
- It is possible to manage oxygen across subsystems to reduce utility demand.
- It is possible to increase production capacity via CAES/TES integration.
- It is possible to enhance techno-economics by co-producing liquid and gaseous fuels.
- It is possible to lower LCA impacts using renewable energy rather than the grid mix.

These results identify practical integration strategies that lift efficiency, cut costs, and reduce environmental footprints in hydrogen-driven polygeneration.

#### 3. Overall key performance indicators

Fuel production capacity anchors plant scale and mass—energy balances, enabling comparison of configurations against targeted outputs. Defined as the sustained rate of saleable fuel under specified conditions, it determines whether a facility is small, medium, or large. Subsystem energy efficiency captures thermodynamic gains from integration and links design choices to lower material use per unit product. It is assessed as the ratio of useful-output energy to input energy [6]:

$$\eta_{\rm en} = \frac{(\dot{m} \cdot LHV)_{\rm P}}{\dot{W}_{\rm in} + (\dot{m} \cdot LHV)_{\rm F}} \tag{1}$$

where  $\dot{m}$ , LHV, and  $\dot{W}_{\rm in}$  denote mass flow, lower heating value, and power input; subscripts P and F index product and fuel streams.

Levelized cost of fuel (LCOF) is the discounted, per-unit cost of producing fuel over a plant's lifetime, enabling comparison across pathways and scales, defined as follows [7]:

$$LCOF = \frac{\left(FCI \cdot CRF + TPC - AI_{Byproducts}\right)}{\dot{m}_{F} \cdot \tau} \tag{2}$$

Here,  $\dot{m}$  is the fuel's mass flow and  $\tau$  is the annual full-load operating hours. FCI, CRF, TPC, and AI denote fixed capital investment, capital recovery factor, total product cost, and annual income, respectively.

Environmental performance is evaluated on a cradle-to-gate basis via *GWP*<sub>100</sub>, reported in kgCO<sub>2</sub>eq/kgFuel, to verify that integration choices deliver decarbonization consistent with EU targets [8]:

$$GWP_{100} = \sum m_i CF_i \tag{3}$$

Where  $m_i$  is the mass of gases in the inventory and  $CF_i$  is the ReCiPe-implemented characterization factor.

Fossil resource scarcity (FDP) measures dependence on fossil inputs. Under ReCiPe 2016, extracted carriers (oil, gas, coal) are converted to oil-equivalent mass via fossil fuel potential factors and summed [9]:

$$FDP = \sum R_j CF_j \tag{4}$$

Where  $R_j$  is the quantity of fossil resources and  $CF_j$  is based on the ratio of the carrier's higher heating value (HHV) to that of crude oil.

### 4. Proposed scenarios

This section introduces eight scenarios that operationalize the thesis hypothesis: it is possible to raise efficiency, cut costs, and reduce life-cycle burdens by coordinating hydrogen, oxygen, heat, and power within biofuel polygeneration systems. The scenarios span feedstock routes (anaerobic digestion vs. oxygen-steam gasification), product slates (biomethanol, ammonia, and biojet fuel), and electrolyzer choices (alkaline vs. high-temperature SOEC), while activating key integration levers, LNG-gas-turbine energy recovery, WGS membrane configuration, heat management using energy storage, oxygen utilization, and CO2 recycling. Each case is defined on a common functional basis and assessed consistently for energy efficiency, levelized cost, levelized cost, and LCA indicators (GWP, fossil depletion). Together, the eight scenarios map the design space for hydrogen-enabled power-/biomass-to-X systems and identify practicable configurations where immediate hydrogen use maximizes decarbonization and deployment readiness.

# 4.1. Power and biogas to methanol

The base case shown in Fig. 2 integrates high-temperature electrolysis with sewage-sludge anaerobic digestion to convert low-value residues and renewable electricity into biomethanol and biomethane. Biogas is upgraded to biomethane while the separated CO<sub>2</sub> is combined with SOEC-derived H<sub>2</sub> for compressed, looped methanol synthesis and final distillation; process water is recycled to the electrolyzer and cooler waste heat supplies steam, closing heat and water loops. Operable on wind power or the Polish grid, this configuration provides an efficient, environmentally favorable reference for subsequent optimization.

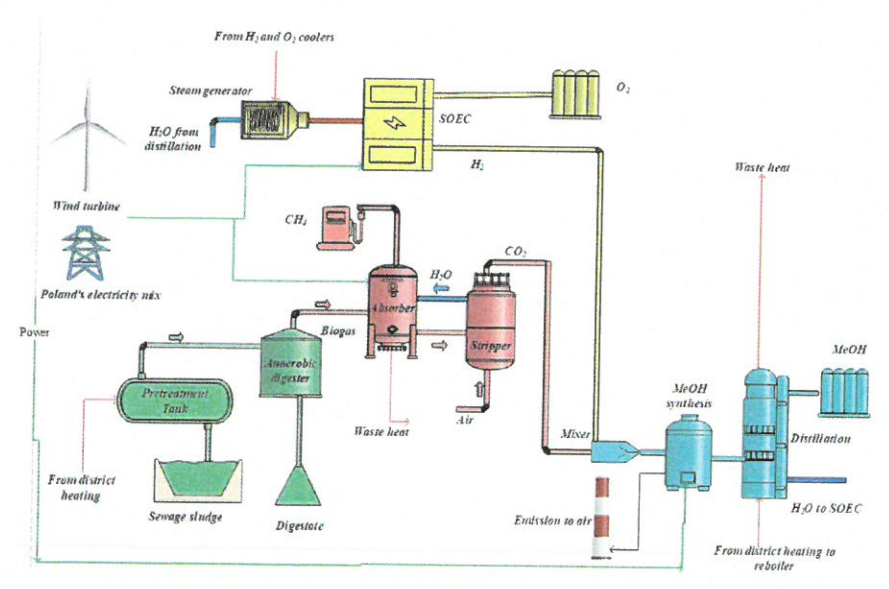


Fig. 2. Base case for biomethanol production.

Figure 2 reveals a baseline biomethanol scheme with major integration gaps, such as low-temperature waste heat being dumped, electrolytic O<sub>2</sub> being vented or requiring storage, and weak thermal coupling, which raises energy use and costs. Figure 3 addresses these limits by integrating LNG regasification, an oxy-fuel gas turbine, and a water-gas-shift reactor with the SOEC and methanol loop. Methanol-loop waste heat is harnessed to offset LNG cold duty. By-product O<sub>2</sub> feeds oxy-combustion for power, and conditioned flue gases are recycled for CO<sub>2</sub> hydrogenation. This configuration strengthens hydrogen utilization, reduces external utilities, and increases efficiency and fuel capacity, providing a coherent pathway beyond the base case.

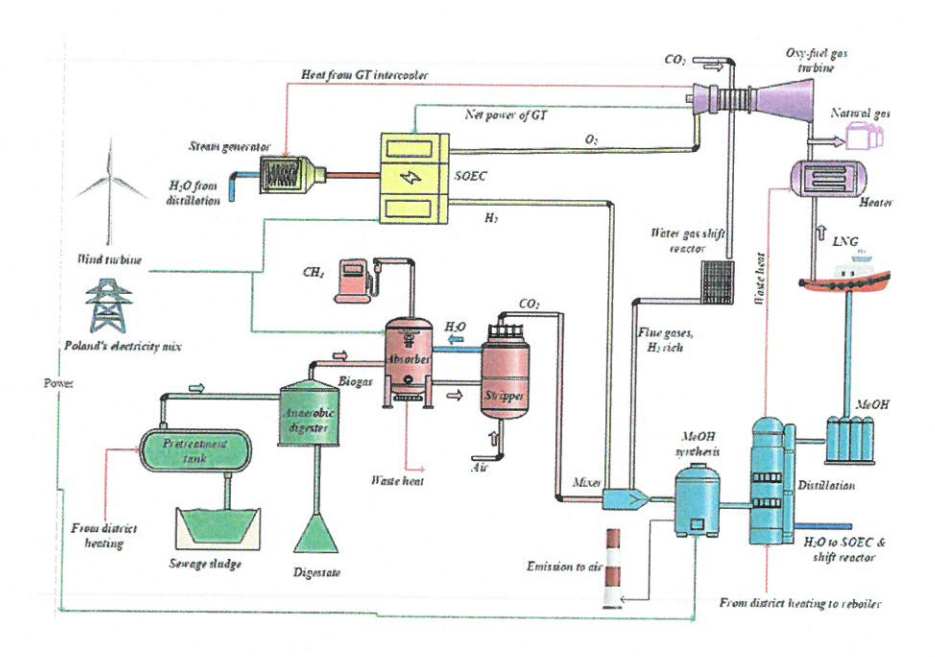


Fig. 3. Improved case of biogas-based biomethanol and natural gas production.

Figure 4 compares the base and improved biogas-based hydrogen schemes, keeping biogas generation and upgrading unchanged, across energy, techno-economic, and life-cycle metrics. A 25-year net present value (NPV) and payback time analysis shows markedly stronger economics for the LNG-gas-turbine integration, with a 3-year payback versus 10 years and an NPV of 140 M\$ versus 20 M\$. Gains stem from added natural-gas co-production (2.5 tonne/h), higher biomethanol output, and reduced purchased electricity, confirming that LNG-GT coupling enhances revenue, capital recovery, and deployment readiness of the hydrogen-enabled polygeneration system.

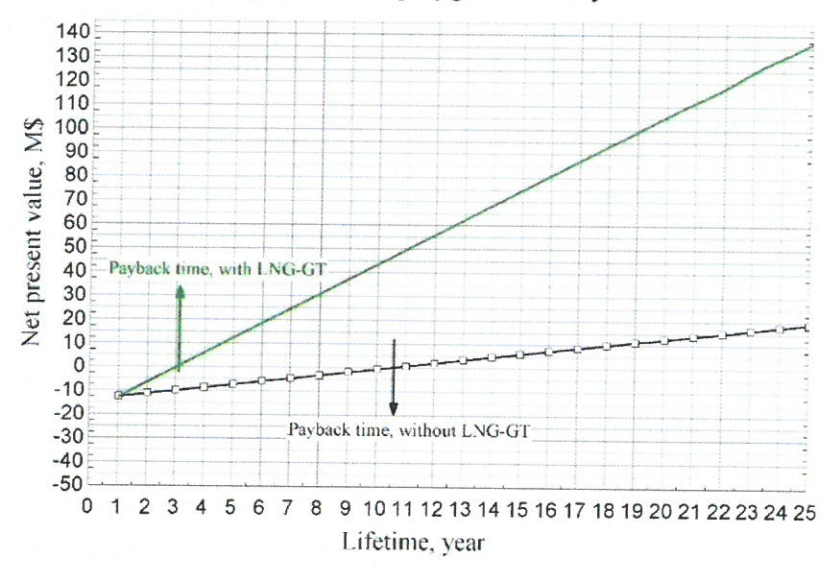


Fig. 4. The lifetime impact on the plant's NPV with and without LNG-GT subsystems.

Figure 5 presents the consequential LCA, indicating that integrating LNG regasification and a gas turbine reduces environmental burdens compared to the base case. The LNG–GT configuration achieves 53% lower climate impact by co-producing domestic natural gas that displaces imports and associated transport emissions. These results validate the hypothesis that energy integration outperforms the base design on environmental metrics.

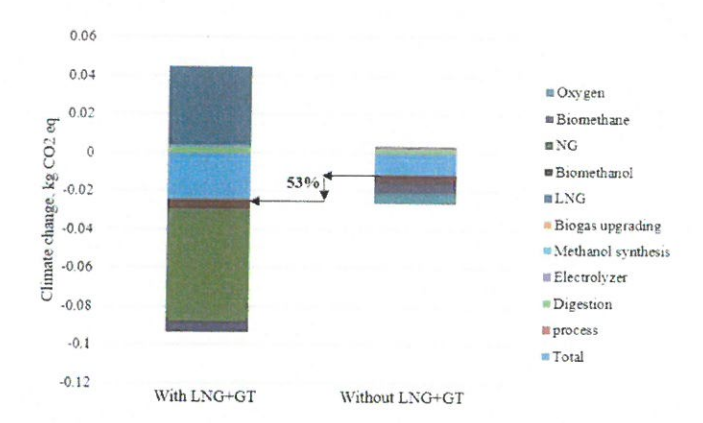


Fig. 5. Comparison of the values of climate change with and without LNG and gas turbine subsystems.

# 4.2. Biomass-to-methanol system using gasification

This chapter extends the analysis to an oxygen-steam biomass-to-methanol pathway via wood gasification. Figure 6 summarizes an integrated configuration that couples the gasifier with SOEC (shared high-temperature heat and direct O<sub>2</sub> use), a methanol synthesis loop, LNG cold-energy recovery, an oxy-fuel gas turbine, steam generators, and a shift reactor. Waste-heat is routed to the SOEC, methanol-loop heat is valorized against LNG regasification, SOEC-derived O<sub>2</sub> serves both gasification and oxy-combustion, and shifted flue gas is recycled for CO<sub>2</sub> hydrogenation, raising hydrogen utilization while co-producing biomethanol and natural gas and reducing external utilities.

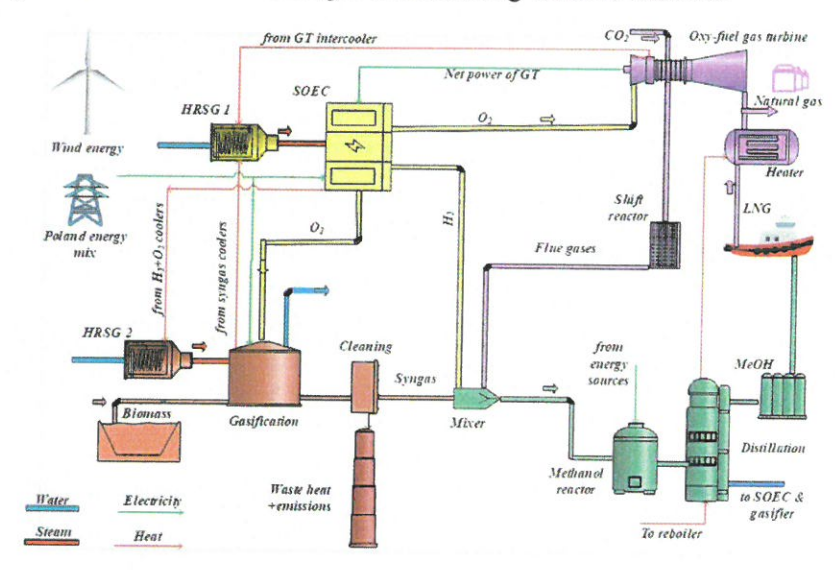


Fig. 6. Schematic diagram of the proposed cycle to produce natural gas and biomethanol using biomass gasification.

# 4.3. Biomass-to-methanol with energy storage

This configuration integrates biomass gasification, SOEC, methanol synthesis, Compressed airthermal energy storage (CAES/TES), power generation, and natural-gas production, tightly coupled via LNG cold-energy recovery to close heat and oxygen loops. As shown in Fig. 7, methanol-loop waste heat is valorized against LNG regasification, high-temperature heat is routed to the SOEC and HRSGs, and surplus O<sub>2</sub> drives an oxy-turbine; a shift reactor conditions flue gas that is recycled with syngas and H<sub>2</sub> to synthesize additional methanol. CAES supplies recoverable compressor heat to TES, which smooths the transient operation and delivers steady process heat to the biofuels plant. Overall, the scheme raises hydrogen utilization, reduces external utilities, and expands co-production of biomethanol and natural gas.

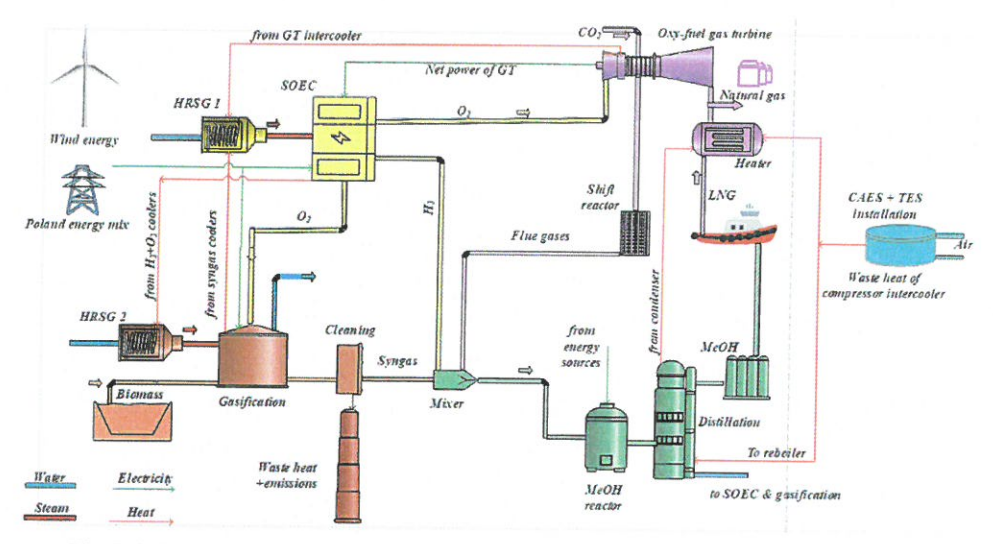


Fig. 7. Schematic diagram of the proposed cycle to produce natural gas and biomethanol.

# 4.4. Ammonia production plants

This chapter tests the hydrogen-use hypotheses for a second flagship product, ammonia, by benchmarking three routes under consistent assumptions: power-to-ammonia (PtA) and biomass-to-ammonia (BtA) with co-current and counter-current WGS. Fig. 8 summarizes the block-flow layouts and the PtA process flow: solar-PV power drives alkaline electrolysis for  $H_2$ , an air separation unit supplies  $N_2$  for Haber–Bosch process, and  $O_2$  is exported.

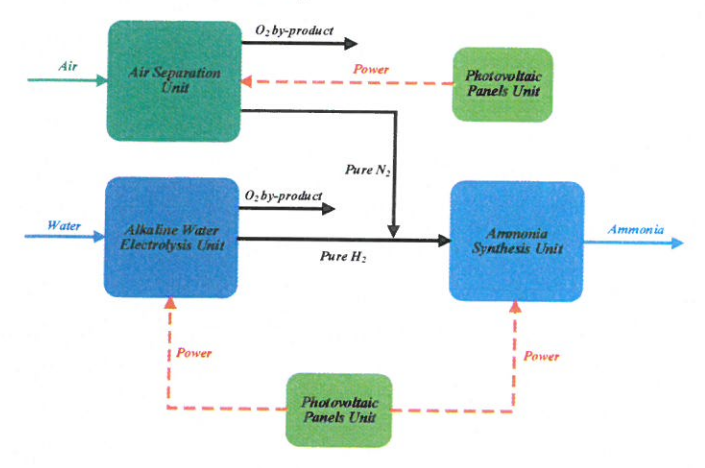


Fig. 8. Process flow diagram of the PtA plant.

Biomass-to-ammonia (BtA) replaces electrolytic H<sub>2</sub> with gasification-derived syngas conditioned in membrane-assisted WGS. This thesis benchmarks concurrent and counter-current variants (Fig. 9), utilizing PV power, an air separation unit that supplies N<sub>2</sub> for the Haber–Bosch process and O<sub>2</sub> for gasification, and a CCS block that captures WGS off-gas to store liquid CO<sub>2</sub>. Permeate H<sub>2</sub> feeds the synthesis loop while retentate is combusted prior to capture.

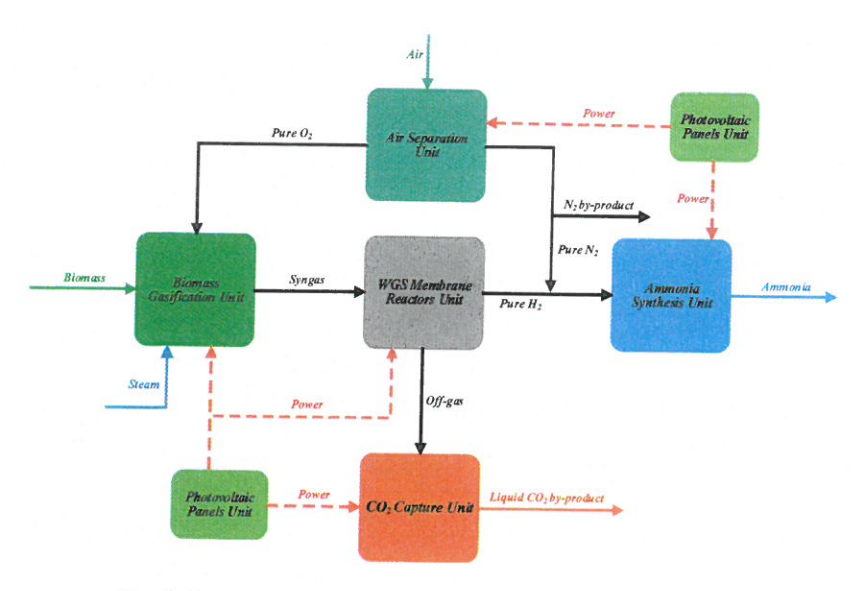


Fig. 9. Process flow diagram of the biomass-to-ammonia plants/

# 4.5. Biojet fuel production system

This chapter extends the thesis to sustainable aviation fuel (SAF) by proposing a hydrogen-enabled biomass-to-jet pathway that co-integrates oxygen-blown gasification, high-temperature SOEC, Fischer—Tropsch (FT) synthesis, and LNG-gas-turbine (GT) energy recovery. As outlined in Fig. 10, high-temperature coupling of SOEC and gasification supplies steam and valorizes O<sub>2</sub> for gasification and oxy-GT power, while low-temperature pairing of FT waste heat with LNG regasification recovers cold duty and trims external utilities; cleaned syngas and SOEC H<sub>2</sub> feed FT, with flue-gas recycling further boosting conversion. The scheme is evaluated under wind power versus the Poland electricity mix to test power-source sensitivity. Together, these integrations aim to deliver efficient, lower-impact, and deployable SAF co-produced with natural gas, validating the thesis hypotheses in a hard-to-abate sector.

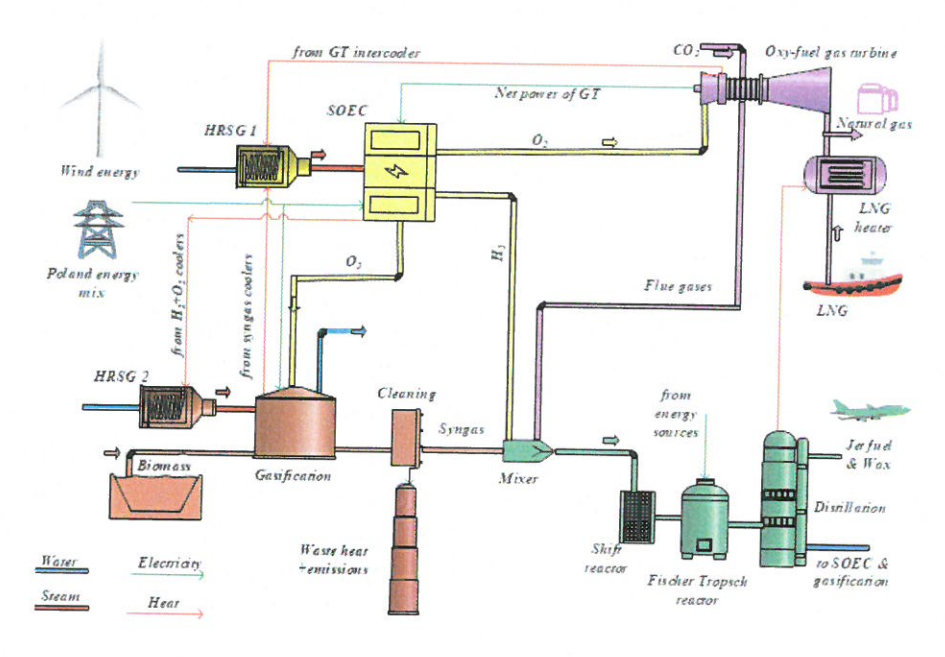


Fig. 10. Schematic diagram of the proposed plant for producing biojet fuel and natural gas.

Figure 11 illustrates that electricity price is the primary driver of hydrogen-enabled SAF economics: the LCOF rises roughly linearly with power cost, while the payback grows steeply, reflecting

the compounding of operating costs. When using Poland electricity mix, the plant achieves cost parity and is economically feasible. Sensitivity results indicate that using the Polish electricity mix yields lower LCOF and shorter payback than wind power, making it the more viable option under the assumed price conditions.

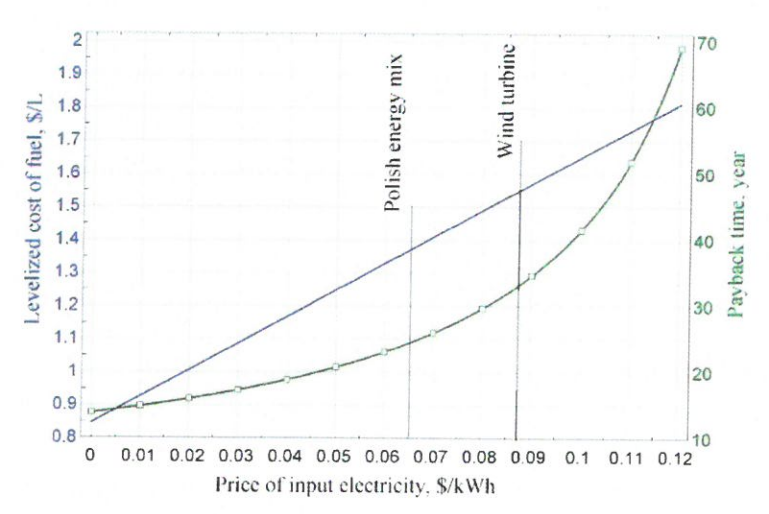


Fig. 11 Analysis of the influence of the electricity price on the levelized cost of fuel and the payback time.

Figure 12 explains how the electricity supply governs the life cycle GHG footprint of the SAF pathway. Contrasting Poland electricity mix with wind energy directly tests the hypothesis that renewable sourcing lowers impacts in hydrogen-based and electrified plants. In Fig. 12(a), using Poland's electricity mix, 97.3% of the total GWP comes from the Poland energy mix itself, highlighting the heavy dependence on fossil fuels. Minor contributions come from LNG at 1.6%, CO<sub>2</sub> at 0.8%, and biomass at just 0.3%. In contrast, Fig. 12(b) shows that when wind turbines are used, the environmental burden is more balanced. Wind energy accounts for 48.4% of the greenhouse gas (GWP), with LNG contributing 30.8%, CO<sub>2</sub> at 15.1%, and biomass at 5.7%. Although wind energy still represents the largest share in this setup, it is worth noting that this includes its full life cycle impact, from manufacturing to operation and decommissioning. Overall, the comparison clearly shows that producing SAF with wind energy results in a substantially lower environmental footprint compared to using Poland's conventional energy mix. This highlights the crucial role of renewable energy sources in reducing the climate impact of alternative fuels and underscores the need to decarbonize national energy grids for a more sustainable future.

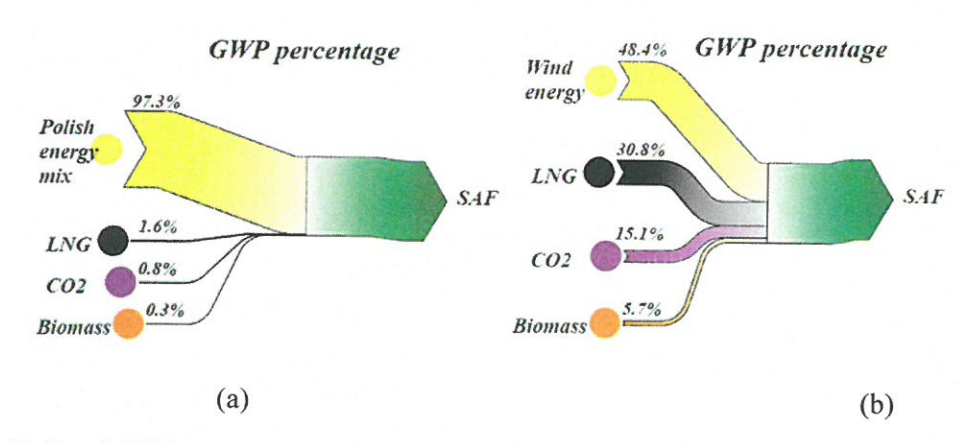


Fig. 12. Overall GWP percentage of the proposed system. a) Poland's electricity mix. b) Wind turbines.

#### 5. Comparison of results

This chapter consolidates the results from eight proposed pathways based on renewable energy, biogas-to-methanol (base and improved), biomass-to-methanol (with and without LNG/energy storage systems), power-to-ammonia, biomass-to-ammonia (CO/CC WGS), and biojet fuel via FT synthesis, into a single comparative assessment to identify the best hydrogen-enabled configuration. It benchmarks common KPIs (energy efficiency, levelized costs, and cradle-to-gate LCA indicators). This comparison directly tests the hypotheses that coordinated use of H<sub>2</sub>, O<sub>2</sub>, heat, and power, together with storage and waste-heat recovery, can deliver superior outcomes. The outcome is a defensible selection of the best system for hydrogen utilization and bio-based fuel/chemical production, plus generalizable design rules to guide optimization.

As presented in Table 1, among the biomethanol options, the improved BtM with energy storage (System 4, as shown in the Table) is the strongest all-around choice for hydrogen utilization due to heat recovery from CAES/TES energy storage and high fuel production. It achieves the highest energy efficiency at 95.27% and the largest fuel capacity at 8062 kg/h, while also posting the lowest environmental burdens among the BtM routes (GWP=0.1346 kgCO2-eq/kgFuel, FDP=0.0254 kgoileq/kgFuel). Its cost, 602.2 \$/tonne, is narrowly above the cheapest case. If minimizing unit cost is the sole criterion, the Improved biogas-based methanol production base integrated with LNG regasification (System 2) is the lowest-cost at 574.4 \$/tonne because biogas plants are cheaper than gasification. It has solid efficiency (84%) and mid-range impacts (GWP 0.2059, FDP 0.0415). The gasification variant (System 3) trails on cost (961 \$/tonne) and efficiency (81.96%). Relative to fossil market methanol (1100 \$/tonne,  $\eta = 71\%$ , GWP 0.908, FDP 0.907), both System 2 and System 4 are decisively superior: System 4 cuts GWP by 85% and FDP by 97% while lifting efficiency by 24.3%, and System 2 remains 48% cheaper than fossil with markedly lower impacts. In the context of the thesis objective, optimizing hydrogen utilization through deep thermal and process integration, System 4 is the preferred design, translating high-temperature SOEC integration and CAES/TES heat recovery into the highest conversion of input H2 into saleable biomethanol at the lowest environmental cost.

For ammonia production, the improved BtA (System 7) configuration, which utilizes biomass gasification and a counter-current WGS membrane, is the best-balanced option. At essentially the same plant capacity (83472 kg/h), it delivers the highest energy efficiency among the green ammonia options (54.64%), the lowest LCOF (513.28 \$/tonne), and the lowest environmental burdens (GWP=0.175 kgCO<sub>2</sub>-eq/kgFuel, FDP = 0.046 kgoileq/kgFuel). The PtA route using alkaline electrolysis is weaker on all KPIs, and the Basic BtA (with co-current WGS) lags on both efficiency (51.60%) and cost (562.98 \$/tonne). Against fossil market ammonia, the Improved BtA cuts GWP by 93% and FDP by 95% while also being 46% cheaper on LCOF. In the context of optimizing hydrogen utilization, the counter-current membrane WGS in the improved BtA maximizes H<sub>2</sub> recovery from syngas, translating into the best energy—cost—emission performance among the ammonia options.

For biojet fuel production, the proposed gasifier, SOEC, LNG route is the clear winner across all KPIs and outperforms fossil jet fuel on every axis. It delivers a fuel capacity of 3949 kg/h, the highest energy efficiency (56.21%), the lowest LCOF (1893 \$/tonne), and markedly better environmental metrics, GWP = 0.464 kgCO<sub>2</sub>eq/kgFuel (50% lower than that of fossil jet fuel) and FDP = 0.3233 kgoileq/kgFuel (73% lower than 1.2 for fossil-based). These improvements align directly with the thesis aim of optimizing hydrogen utilization: high-temperature SOEC hydrogen is used to upgrade biogenic syngas in FT synthesis while LNG/GT energy recovery tightens integration, raising conversion efficiency and cutting both cost and life-cycle burdens.

Table 1. Comparison of the results of all proposed systems for hydrogen utilization.

System	Subsystems	$m_F$ , kg/h	$\eta$ , %	LCOF, \$/tonne	GWP, kgCO2eq/kgFuel	FDP, kgoileq/kgFue
-	Biomethanol production					
1-Basic BtM	Anaerobic digestion, biogas upgrading, SOEC, methanol synthesis	366	64.55	633.7	-	-
2- Improved BtM	Anaerobic digestion, biogas upgrading, SOEC, methanol synthesis, LNG-GT	2893	84	574.4	0.2059	0.0415
3- Improved BtM using gasification	Gasifier, SOEC, MeOH, LNG-GT	2061	81.96	961	0.1666	0.0345
4- Improved BtM using energy storage	Gasifier, SOEC, MeOH, LNG-GT, CAES/TES	8062	95.27	602.2	0.1346	0.0254
-	Market MeOH [10], [11], [12]	-	71.00	1100	0.908	0.907
-	Ammonia production					
5- PtA	Air separation, Alkaline electrolyzer, Ammonia synthesis	83399	50.19	540.77	0.772	0.201
6- Basic BtA	Air separation, Biomass gasification, CO-WGS, Ammonia synthesis, CCS	83472	51.60	562.98	-	-
7- Improved BtA	Air separation, Biomass gasification, CC-WGS, Ammonia synthesis, CCS	83472	54.64	513.28	0.175	0.046
-	Market Ammonia [10], [13]	-	66.36 (Exergy- based)	950	2.66	0.945
-	Biojet fuel production					
8- Biojet fuel production	Biomass gasification, SOEC, FT synthesis, LNG-GT	3949	56.21	1893	0.464	0.3233
	Market jet fuel [10], [14], [15]		49.9 (for SAF)	2694	0.923	1.2

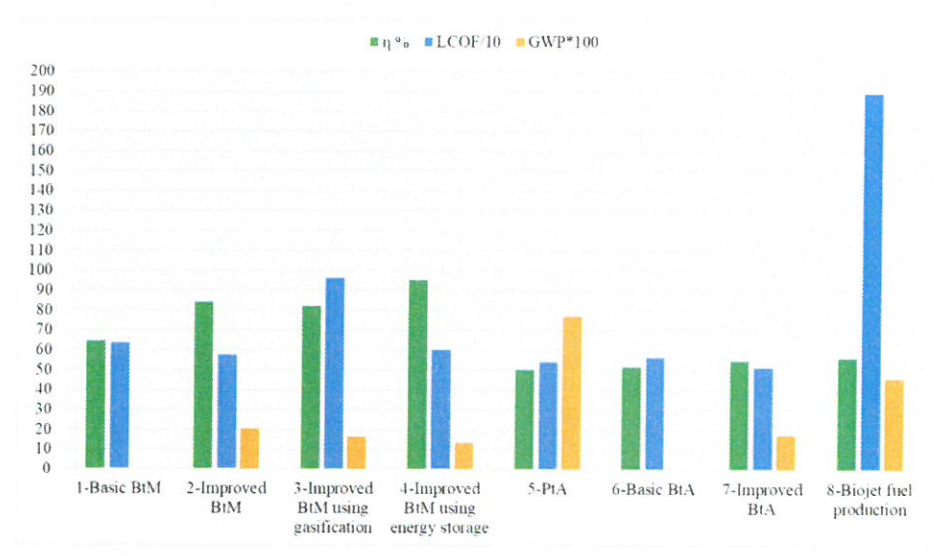


Fig. 13. Results comparison of all proposed systems for hydrogen utilization.

The bar chart presented in Fig. 13 compacts the same data as Table 1 but plots only the three decision KPIs, overall energy efficiency ( $\eta$ ), levelized cost of fuel (LCOF divided by 10), and climate impact (GWP, scaled ×100). Three plants stand out as the most optimal configurations for hydrogen utilization.

Overall, the comparison recommends leveraging the following subsystems to optimize hydrogen utilization across energy, techno-economic, and life-cycle assessment (LCA) performance:

- Biomass gasification with combined O<sub>2</sub>/steam agents,
- High-temperature SOEC for maximum efficiency, and low-temperature ALE for costeffectiveness.
- Counter-current water-gas shift (WGS) membrane reactor,
- Integrated heat recovery among the LNG-gas turbine (LNG-GT), CAES/TES storage, and fuel-synthesis loops,
- Coordinated O<sub>2</sub>/CO<sub>2</sub> management across subsystems.

#### 6. Conclusions

Hydrogen, treated as a unifying energy carrier and design variable, enables rigorous optimization of polygeneration systems that co-produce liquid and gaseous fuels while balancing efficiency, cost, and environmental performance. This thesis integrates thermodynamic modeling with techno-economic assessment and life-cycle analysis across eight novel routes, including biogas-to-methanol, two biomass-to-methanol configurations (with LNG heat recovery and energy storage systems), three ammonia scenarios, and biojet fuel production. The result is a coherent framework and a set of generalizable design rules showing how electrolyzer-centric heat, O<sub>2</sub>, and H<sub>2</sub> utilization, targeted separations, and strategic co-production reshape plant-level trade-offs and push bio-based fuels toward lower emissions and economic feasibility. The main conclusions of the thesis can be summarized as follows:

- Chemical storage of liquid biofuels is easier and safer than compressed/cryogenic H<sub>2</sub> gas storage.
- High-temperature electrolysis cell (SOEC) enables energy-synergistic heat and power integration, delivers O<sub>2</sub> to displace air separation, and supplies H<sub>2</sub> to produce biomethanol, ammonia, and biojet fuel, collectively lifting system efficiency.
- The ammonia cases highlight that the least-cost PtA with alkaline electrolyzer is not the most energy-efficient, while biomass-to-ammonia with membrane WGS maximizes efficiency.
- Counter-current WGS membrane reactors consistently outperform co-current designs on H<sub>2</sub> recovery and overall efficiency. LNG cold energy recovery and oxy-fuel gas turbines reduce net power demand.
- Cogeneration of biomethanol and natural gas with O<sub>2</sub>/CO<sub>2</sub> management shortens payback time and increases robustness to electricity-price volatility compared with single-product plants.
- Electrolyzer and fuel-synthesis units dominate capital costs. Therefore, electricity price and sourcing are first-order determinants of levelized cost across all pathways.
- Wind energy significantly reduces cradle-to-gate GHG emissions and fossil resource depletion relative to the Poland electricity mix. Process intensification (oxy-gas turbine with CO<sub>2</sub> injection, LNG cold-energy recovery) further improves footprints.
- SOEC is preferred when high-temperature integration is feasible.
- A counter-current WGS membrane reactor is selected for the production of ammonia.
- LNG cold-energy recovery and oxy-combustion are included when grid relief and flue-gas recycling are priorities.

- Cogeneration of natural gas and biofuels is advantageous when electricity prices are high or volatile.
- Renewable energy is chosen when environmental sustainability is prioritized.
- Compressed air and thermal energy storage modules convert transient waste heat into a steady biomethanol product, reducing grid variability and enhancing efficiency enhancement.
- Design optimization workflow yields decision-ready trade-off maps for efficiency, cost, and emissions based on heat-power integration, electrolyzer placement/sizing, and subsystems coupling with techno-economic and LCA feedback.
- The improved BtM with CAES/TES is the overall optimum for hydrogen utilization, highest efficiency (95%), competitive cost (602 \$/tonne), and the lowest GWP (0.135 kgCO<sub>2</sub>eq/kgFuel), validating the thesis on high-temperature, deeply integrated heat recovery around SOEC, gasification, and LNG.
- For ammonia, the BtA route with counter-current membrane WGS is preferred, with an acceptable efficiency (54.6%), the lowest cost among all plants (513 \$/tonne), and near-zero GHG intensity (0.175 kgCO<sub>2</sub>eq/kgFuel) due to superior H<sub>2</sub>/O<sub>2</sub> and N<sub>2</sub> management.
- The biojet pathway remains strategically important for hard-to-electrify aviation (efficiency 56%, cost 1893 \$/tonne, GWP 0.464 kgCO2eq/kgFuel).
- Optimal hydrogen utilization emphasizes O<sub>2</sub>/steam gasification, high-temperature SOEC (with ALE as a cost lever), counter-current WGS membranes, integrated heat recovery between LNG-GT and CAES/TES, and coordinated O<sub>2</sub>/CO<sub>2</sub> utilization across subsystems.
- The Poland energy mix is a more economically viable option than wind turbines. However, wind energy outperforms Poland's electricity mix in most of the environmental indicators. The reductions are substantial, particularly concerning climate change and fossil resource scarcity, demonstrating the critical role of renewable energy in achieving carbon neutrality and mitigating environmental degradation.

#### References

- [1] "Shedding light on energy in Europe 2025 edition Interactive publications Eurostat." Accessed: Aug. 28, 2025. [Online]. Available: https://ec.europa.eu/eurostat/web/interactive-publications/energy-2025?utm\_source=chatgpt.com#energy-sources
- [2] "How Does Anaerobic Digestion Work? | US EPA." Accessed: Aug. 29, 2025. [Online]. Available: https://www.epa.gov/agstar/how-does-anaerobic-digestion-work
- [3] N. Johnson, M. Liebreich, D. M. Kammen, P. Ekins, R. McKenna, and I. Staffell, "Realistic roles for hydrogen in the future energy transition," *Nature Reviews Clean Technology 2025 1:5*, vol. 1, no. 5, pp. 351–371, Apr. 2025, doi: 10.1038/s44359-025-00050-4.
- [4] T. International Renewable Energy Agency, "green hydrogen cost reduction scaling up electrolysers to meet the 1.5°c climate goal h 2 o 2," 2020.
- [5] "Safety, Codes and Standards | Department of Energy." Accessed: Aug. 29, 2025. [Online]. Available: https://www.energy.gov/eere/fuelcells/safety-codes-and-standards
- [6] H. Ghiasirad and A. Skorek-Osikowska, "Parametric analysis of biomethanol production unit using biomass gasifier and high-temperature electrolyzer," *Proceedings of WHEC 2022 23rd*

- World Hydrogen Energy Conference: Bridging Continents by H2, pp. 252–254, 2022, Accessed: Sep. 16, 2025. [Online]. Available: https://www.scopus.com/pages/publications/85147194871[7] M. Ostadi, L. Bromberg, D. R. Cohn, and E. Gençer, "Flexible methanol production process using biomass/municipal solid waste and hydrogen produced by electrolysis and natural gas pyrolysis," Fuel, vol. 334, Feb. 2023, doi: 10.1016/j.fuel.2022.126697.
- [8] T. F. Stocker et al., "Climate Change 2013 The Physical Science Basis: Working Group I Contribution to the Fifth Assessment Report of the Intergovernmental Panel on Climate Change," Climate Change 2013 the Physical Science Basis: Working Group I Contribution to the Fifth Assessment Report of the Intergovernmental Panel on Climate Change, vol. 9781107057999, pp. 1–1535, Jan. 2014, doi: 10.1017/CBO9781107415324.
- [9] R. Frischknecht *et al.*, "Swiss Centre for Life Cycle Inventories A joint initiative of the ETH domain and Swiss Federal Offices Implementation of Life Cycle Impact Assessment Methods Data v2.0 (2007)," 2007, Accessed: Sep. 06, 2025. [Online]. Available: www.ecoinvent.org[10] "SimaPro Sustainability insights for informed changemakers." Accessed: Sep. 11, 2025. [Online]. Available: https://simapro.com/
- [11] C. Arnaiz del Pozo, S. Cloete, and Á. Jiménez Álvaro, "Techno-economic assessment of long-term methanol production from natural gas and renewables," *Energy Convers Manag*, vol. 266, p. 115785, Aug. 2022, doi: 10.1016/J.ENCONMAN.2022.115785.[12] Z. Zhang, B. Delcroix, O. Rezazgui, and P. Mangin, "Simulation and techno-economic assessment of bio-methanol production from pine biomass, biochar and pyrolysis oil," *Sustainable Energy Technologies and Assessments*, vol. 44, Apr. 2021, doi: 10.1016/j.seta.2021.101002.[13] S. Mingolla *et al.*, "Effects of emissions caps on the costs and feasibility of low-carbon hydrogen in the European ammonia industry," *Nature Communications 2024 15:1*, vol. 15, no. 1, pp. 1–23, May 2024, doi: 10.1038/s41467-024-48145-z.
- [14] M. Hillestad *et al.*, "Improving carbon efficiency and profitability of the biomass to liquid process with hydrogen from renewable power," *Fuel*, vol. 234, pp. 1431–1451, Dec. 2018, doi: 10.1016/j.fuel.2018.08.004.
- [15] M. Dossow, V. Dieterich, A. Hanel, H. Spliethoff, and S. Fendt, "Improving carbon efficiency for an advanced Biomass-to-Liquid process using hydrogen and oxygen from electrolysis," *Renewable and Sustainable Energy Reviews*, vol. 152, Dec. 2021, doi: 10.1016/j.rser.2021.111670.